Silicon (2023) 15:5233–5243
https://doi.org/10.1007/s12633-023-02433-3

RESEARCH

Thermal and Mechanical Studies of Cerium Molybdenum Borosilicate Glasses and Glass–Ceramics

Kh. S. Shaaban[1] · B. M. Alotaibi[2] · Z. A. Alrowaili[3] · M. S. Al-Buriahi[4] · A. Ashour[5] · Sayed Yousef[6,7]

Received: 15 February 2023 / Accepted: 23 March 2023 / Published online: 29 March 2023

Abstract

This investigation will focus on a particular molybdenum borosilicate glass with the form $61B_2O_3$ – $19SiO_2$- (20-x) MoO_3—x CeO_2, x = (0 ≤ x ≤ 12 mol. %). DTA examination was conducted using a Shimadzu -DTA equipment. The powder glass samples (10 mg) were placed in a platinum pan and heated to 800 °C in nitrogen medium at various rates. The temperatures of the glass transition, T_g, the crystallization extrapolated onset, T_c, the crystallization peak, T_P, and melting T_m, were determined. The quantity of CeO_2 in the checked glass had a significant impact on its crystallization behavior, with an increase in CeO_2 content increasing ΔT and thus making the glasses more stable. With increasing CeO_2 concentrations, both E_G & E_c values decrease, as expected given the rise in T_g & T_P values. XRD and SEM were used to identify the crystallizing phases and microstructural morphology for each composition. Based on XRD observations, Molybdenum Silicide (Mo_3Si_2), Molybdenum Boride (B_2Mo_1), Cerium Borate ($B_1Ce_1O_3$), Cerium Molybdenum Oxide ($Ce_{16}Mo_{21}O_{56}$) and Cerium Silicide Oxide ($Ce_{10}O_3Si_8$) phases were detected. The presence of particles with different shapes in both compositions was revealed by SEM micrographs. As CeO_2 concentrations increased, the ultrasonic velocities & elastic moduli increased.

Keywords CeO_2 · Borosilicate · DTA · Crystallization · Hardness

1 Introduction

Uniformity, good stability, greater chemical resistance, and optical transparency are all advantages of borosilicate glass [1–10]. Borosilicate glasses can be employed as a laser host by doping them with rare earth ions (REis) because of their fascinating features [11–22]. An extensive study has been conducted on (REis) -containing glasses. As a result, numerous glasses containing various (REis) have been developed. Specific implementations have been shown to support from CeO_2 glasses [23–25]. The structure of CeO_2-B_2O_3- SiO_2-MoO_3 glass system has yet to be determined, according to the researchers' knowledge. FT-IR Spectra was used to investigate the structure of silicate, borosilicate and aluminosilicate glasses containing CeO_2. With increasing CeO_2 concentration, CeO_4, also increases [23–25].

Qingshun Shi et.al [26]. investigated the structure and chemical stability of La_2O_3 and CeO_2 doped calcium iron phosphate glasses. Impacts of Ce^{+3} on La_2O_3: Ce^{+3} phosphors were investigated by M. Ajmal et al. [27] Ce^{+3} is observed to be more uniformly distributed in borosilicate glass, with no clustering. This study investigated the characterization of CeO_2 was replaced by MoO_3 at various doping ratios. There two valance states of MoO_3 in glasses: Mo^{+5} and Mo^{+6}.In the thermal and optics industries, glasses containing MoO_3 have become important materials. Crystallization is a crucial topic in both glass science and technology. Although crystallization is usually undesirable when making glass, it is a significant procedure for preparing glass ceramics under controlled conditions [28–34].

✉ Kh. S. Shaaban
khamies1078@yahoo.com

1 Chemistry Department, Faculty of Science, Al-Azhar University, P.O. Box 71524, Assiut, Egypt

2 Physics Department, College of Science, Princess Nourah Bint Abdulrahman University, P.O. Box 84428, Riyadh 11681, Saudi Arabia

3 Physics Department, College of Science, Jouf University, P.O. Box: 2014, Sakaka, Saudi Arabia

4 Department of Physics, Sakarya University, Sakarya, Turkey

5 Physics Department, Faculty of Science, Islamic University, P. O. Box 170, Al Madinah, Saudi Arabia

6 Physics Department, Faculty of Science, King Khalid University, P. O. Box 9004, Abha 61413, Saudi Arabia

7 Research Center for Advanced Materials Science (RCAMS), King Khalid University, P. O. Box 9004, Abha 61413, Saudi Arabia

We decided to use a new vitreous matrix, B_2O_3-SiO_2-MoO_3 containing CeO_2, to learn more about the structure and thermal and crystallization kinetics characteristics of fabricate glass systems. This experiment manufactured CeO_2 co-doped B_2O_3-SiO_2-MoO_3 glasses. The objective of this article is to examine the thermal, mechanical, and crystallization kinetics of the B_2O_3–MoO_3–SiO_2 glass containing CeO_2 using DTA, XRD and SEM.

2 Materials and Methodology

These glasses in Table 1 are taken from [1]. The status of the glasses determined using a Rigaku-Top XRD. DTA examination was conducted using a Shimadzu -DTA equipment. The powder glass samples (10 mg) were placed in a platinum pan and heated to 800 °C in nitrogen medium at various rates. The glass–ceramics were fabricated at T_c for 4 h. Using a scanning electron microscope model A Jeol, the surface morphology of several chosen bulk glass samples is examined (JSM-T20, Tokyo, Japan). The ultrasonic measurements were carried out using a system that included the Echo—graph (Krautkramer model USM3 pulsar/receiver instrument). Archimedes' principle determines the density (ρ) of prepared glass–ceramics. The longitudinal and shear V_L&V_T velocities were determined using this method. Besides the density, the V_L&V_T were used to calculate elastic moduli, longitudinal waves $L = \rho v_l^2$, transverse waves $G = \rho v_t^2$, young's modulus $Y = (1+\sigma)2G$, and bulk modulus $= L - \left(\frac{4}{3}\right)G$. Conductivity of fractal bonds $d = (G/K) * 4$. Hardness; $H = \frac{(1-2\sigma)Y}{6(1+\sigma)}$.

3 Results and Discussion

3.1 Physical Investigations

To ensure that the fabricated samples are in the amorphous phase, XRD were measured. Figure 1 depicts the XRD spectrum of the MBSCe4 sample. While all manufactured glasses have similar XRDs, only this sample's

Table 1 Fabricated glasses with mol.%

Code	B_2O_3	SiO_2	MoO_3	CeO_2
$MBSCe_0$	61	19	20	0
$MBSCe_2$	61	19	18	2
$MBSCe_4$	61	19	14	6
$MBSCe_8$	61	19	12	8
$MBSCe_{10}$	61	19	10	10
$MBSCe_{12}$	61	19	8	12

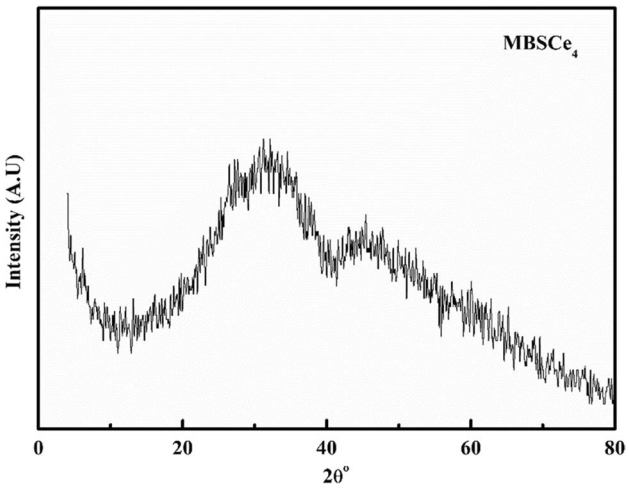

Fig.1 XRD of glass samples

XRD is displayed herein. In their X-ray diffraction patterns, MBSCe4 has broad and diffused humps, indicating that it is amorphous [35–39].

3.2 DTA Examination

T_g, T_c, T_P, and T_m, were determined from DTA [40–50]. For $61B_2O_3 - 19SiO_2$- $(20 - x)$ MoO_3—x CeO_2, glasses, typical DTA are revealed in Fig. 2. The values of $T_g, T_c, T_P and T_m$ for examined samples are presented in Figs. 3(a, b, c and d). These Figs. shows an increasing trend of $T_g, T_c, T_P and T_m$ as CeO_2 content increment. Thermal stability (ΔT) was calculated using the $(T_c - T_x)$ value where T_x is the onset glass transition temperature. For $61B_2O_3 - 19SiO_2$- $(20 - x)$ MoO_3—x CeO_2, glasses, ΔT are revealed in Fig. 4. It was found that ΔT often increases along with an increase in

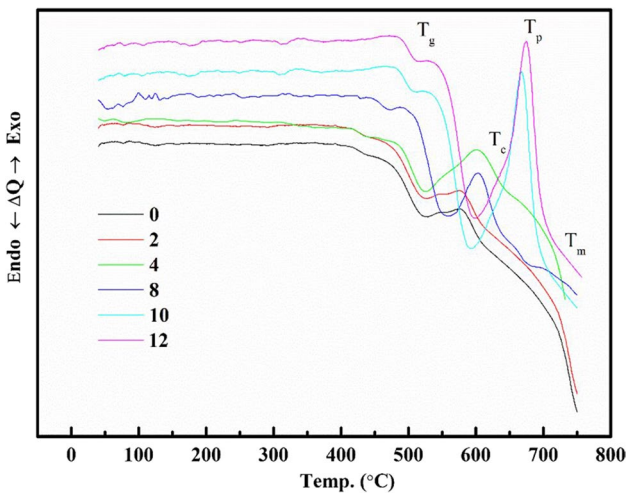

Fig. 2 DTA typical of glass samples

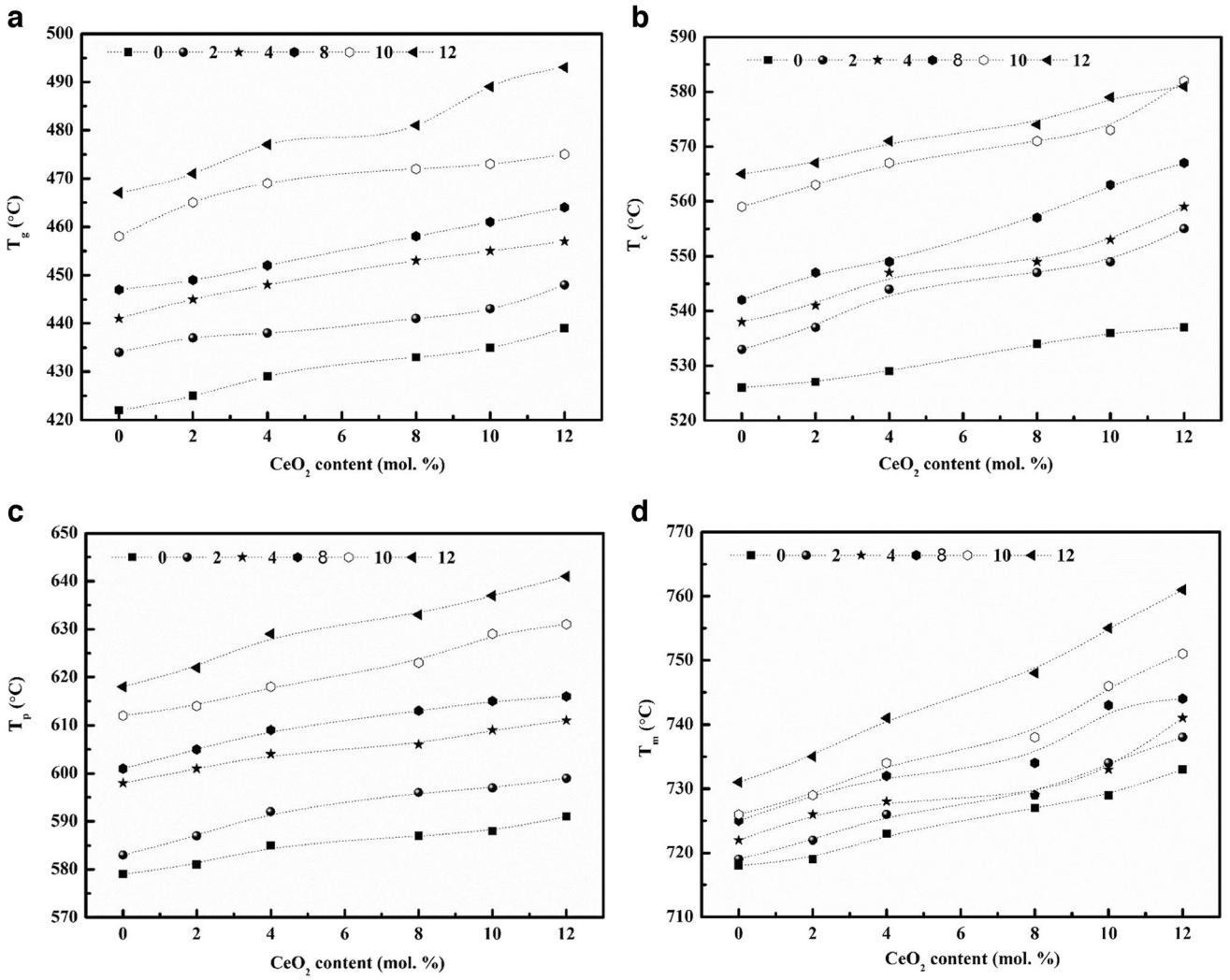

Fig. 3 **a** T_g of the glasses. **b** T_c of the glasses. **c** T_p of the glasses. **d** T_m of glass samples

CeO_2 concentration. With increasing CeO_2 concentration, CeO_4, also increases and the establishment of (BO) increases, therefore ΔT increases (from 88 to 107 °C) as CeO_2 increases. The quantity of CeO_2 in the checked glass had a significant impact on its crystallization behavior, with an increase in CeO_2 content increasing ΔT and thus making the glasses more stable.

Figures 5 and 6 show an increasing trend of weighted thermal stability H_g and S criterion as CeO_2 content increment. $H_g = \frac{\Delta T}{T_g}$, $S = (T_p - T_c)\frac{\Delta T}{T_g}$. This observation due to increase ΔT of the samples. Hruby parameters can be considered as:$H_u = {(T_c - T_g)}/{(T_m - T_c)}$. H_u values for various compositions are shown in Fig. 7. The glass with the highest CeO_2 content is the one that is the most thermally stable.

Lasocka [51] proposed the following expression to describe changes in glass (T_g) and heating rate (β):$T_g = A_g + B_g \ln(\beta)$,

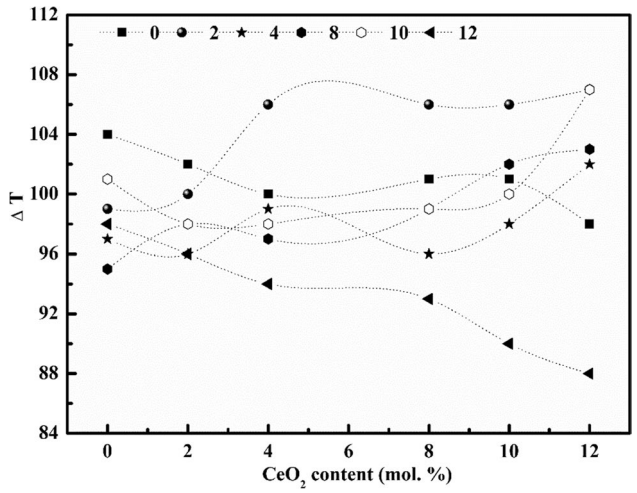

Fig. 4 ΔT of glass samples

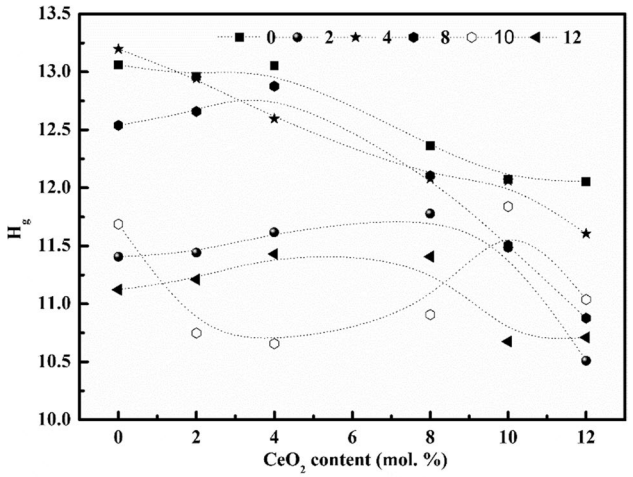

Fig.5 H_g of glass samples

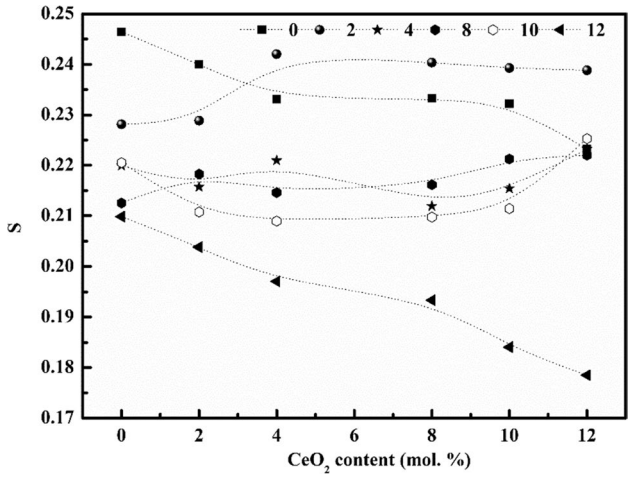

Fig.6 S of glass samples

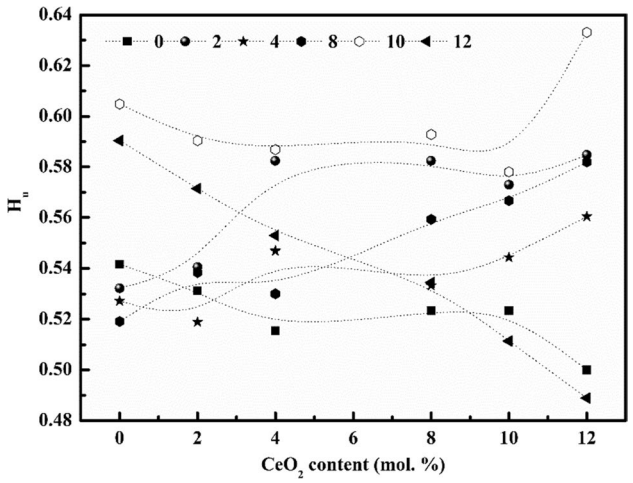

Fig.7 H_u of glass samples

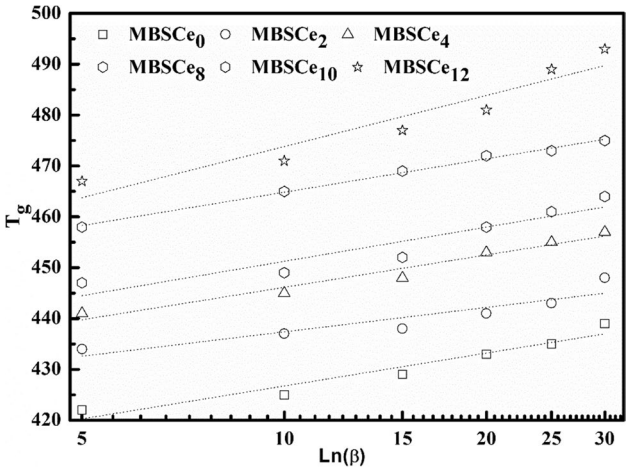

Fig.8 T_g vs.ln(β) for glass samples

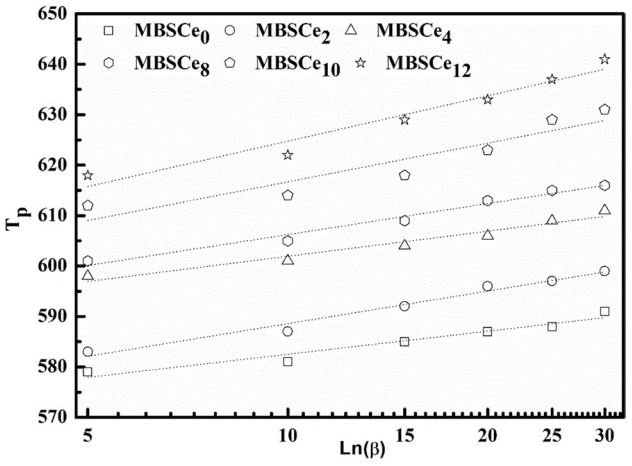

Fig.9 T_p vs.ln(β) for glass samples

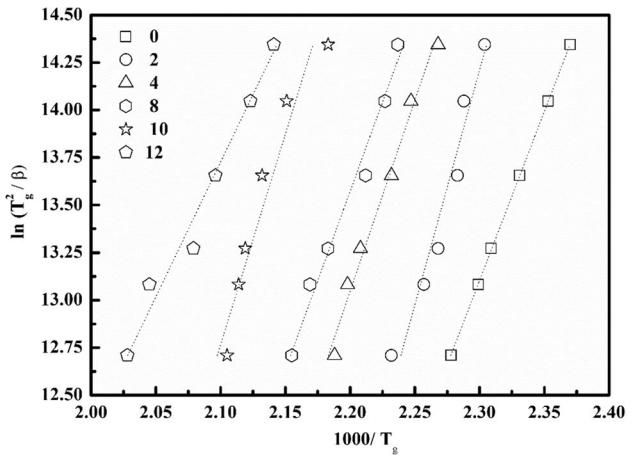

Fig.10 $\ln(T_g^2/\beta)$ versus $10^3/T_g$ for glass samples

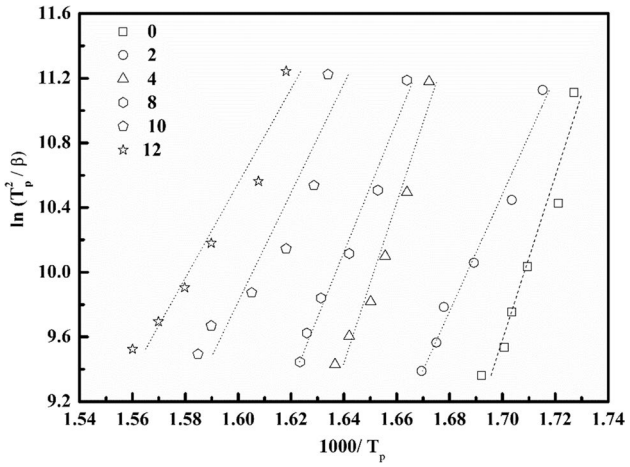

Fig.11 $\ln(T_p^2/\beta)$ versus $10^3/T_p$ for glass samples

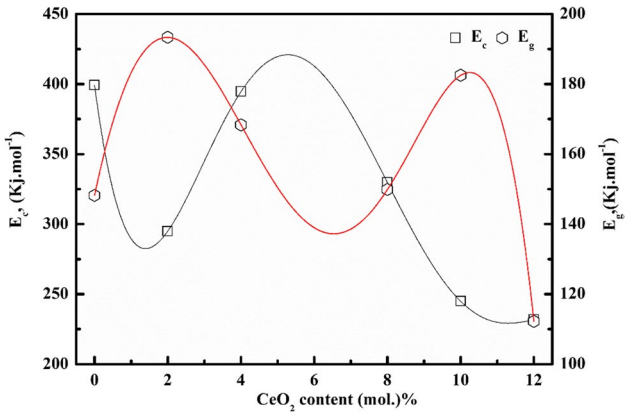

Fig.12 E_G & E_c for glass samples

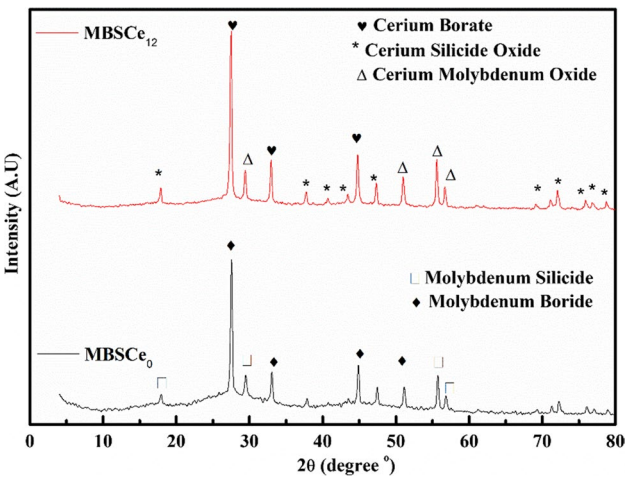

Fig.13 *XRD* for glass–ceramic samples

Table 2 XRD results glass–ceramic samples

Sample	Code	Compound Name Chemical Formula
MBSCe0	98–064-4412	Molybdenum Silicide (Mo_3 Si_2)
	98–007-6410	Molybdenum Boride (B_2 Mo_1)
	98–009-9689	Cerium Borate ($B_1Ce_1O_3$)
MBSCe12	98–007-2525	Cerium Molybdenum Oxide (Ce_{16} Mo_{21} $O5_6$)
	98–017-3576	Cerium Silicide Oxide ($Ce_{10}O_3Si_8$)

which could be used for (T_p) as: $T_p = A_p + B_p \ln(\beta)$, where A_g and A_p are the values of T_g &T_p, respectively. B_g&B_p are constants that depend on the composition of the glass. As shown in Figs. 8 and 9, T_g & T_p values were plotted against ln (β). T_g & T_p values increase with increasing heating rate and CeO_2 concentrations, as shown in these Figs. The observed increase in T_g & T_p values is consistent with previously published data, which can be explained in this way.

Glass transition activation energy E_g, crystallization energy E_c, and the frequency factor k_o, on the other hand, can be easily assigned based on changes in the values of T_g & T_p with (β), as well as the previously described method. Figures 10 and 11 show plots of $\ln(T_g^2/\beta)$ versus $10^3/T_g$ and of $\ln(T_p^2/\beta)$ versus $10^3/T_p$ for investigated samples. The linear relationship of the formula used is represented.

Table 3 XRD investigation of glass–ceramic samples

Sample	Pos 2θ°	Height [cts]	FWHM 2θ°	d-spacing [Å]	Size nm
MBSCe0	27.546	1175.54	0.2362	3.238	121.96
	29.4852	184.18	0.3542	3.03	81.68
	33.0553	265.58	0.2362	2.7	123.55
	44.8794	327.65	0.2362	2.012	128.15
	51.1464	179.35	0.2362	1.786	131.31
	55.7307	290.07	0.2362	1.65	133.98
	56.851	116.45	0.3542	1.62	89.82
MBSCe12	17.8347	205.75	0.3542	4.97348	79.95
	27.4621	2563.83	0.2362	3.24790	121.93
	29.4133	470.04	0.1771	3.03674	163.33
	32.9618	671.30	0.2362	2.71748	123.52
	37.7457	198.32	0.2362	2.38334	125.18
	44.7722	774.55	0.1771	2.02427	170.85
	47.3235	337.96	0.2362	1.92093	129.32
	51	452.13	0.2952	1.79075	105.00
	55.5936	743.33	0.2362	1.65318	133.90
	56.7145	312.61	0.2362	1.62314	134.60
	72.0912	289.78	0.3542	1.31016	97.69
	75.95	96.83	0.7085	1.25291	50.09
	76.9359	84.06	0.4723	1.23930	75.66

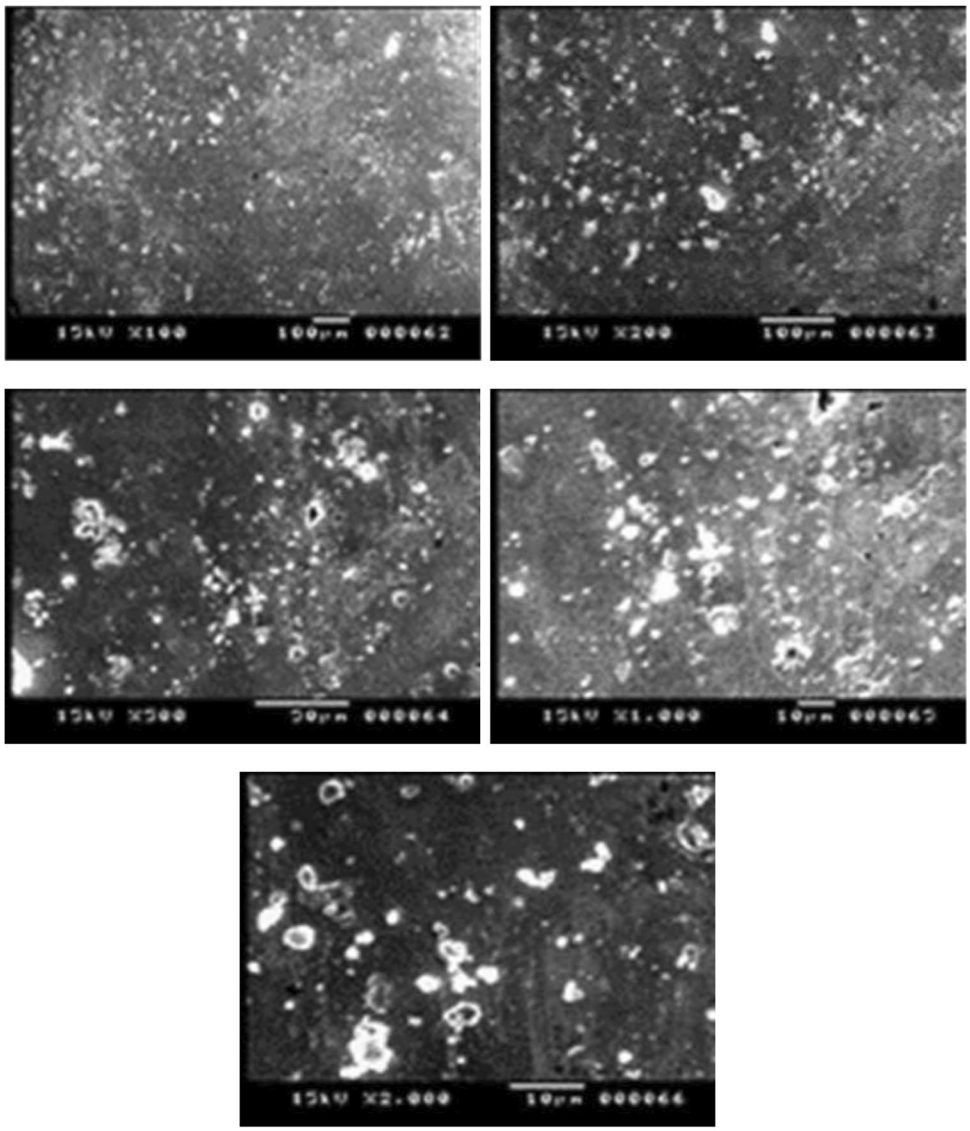

Fig. 14 **a** SEM of $MBSCe_0$ glass -ceramics at magnifications 100, 200, 500, 1000, and 2000. **b**: SEM of $MBSCe_{12}$ glass–ceramics at magnifications 100, 200, 500, 1000, and 2000

Figure 12 shows the values obtained for the glass transition activation energy E_G & E_c. With increasing of CeO_2 concentrations, E_G & E_c values decrease, as expected given the rise in T_g & T_p values. It is predicted that CeO_2 will be transformed into CeO_4 because of the addition of CeO_2. The CeO_4 structural unit has a shorter bond-length than CeO_2, resulting in enhanced bond strength, which could explain why E_G & E_c decrease as CeO_2 content rises.

3.3 Crystallization

The nucleation and growth of crystallites in an amorphous solid is a complicated process that occurs at the same time. MBSCe ceramics samples are chemically resistant and have a variety of applications. Figure 13 shows the XRD of selected ceramic glasses with varying CeO_2 content. In order to identify a structure that appears in X-ray patterns, samples were annealed at temperatures below and above the characteristic points shown in DTA curves. XRD results reveal the formation of crystalline phases as well as an amorphous phase. XRD describe the generated crystalline phases, which were then compared to diffraction patterns of known crystalline compounds containing B, Si, Mo, Ce, and O in the PDF2 database. The XRD for selected samples show a semi-profile. All the expected phases were observed to be present [52–55]. Tables 2 and 3 show the phases and parameters of a variety of glass ceramics.

SEM backscattered of chosen glass–ceramic photographs are shown in Figs. 14a and b. The crystalline surface has a lot of bulky interstitial gaps, revealing the exceptional glass matrix. XRD results support this observation. Microcrystalline extended paths or fibrils, anhedral microcrystals, and a

Fig. 14 (continued)

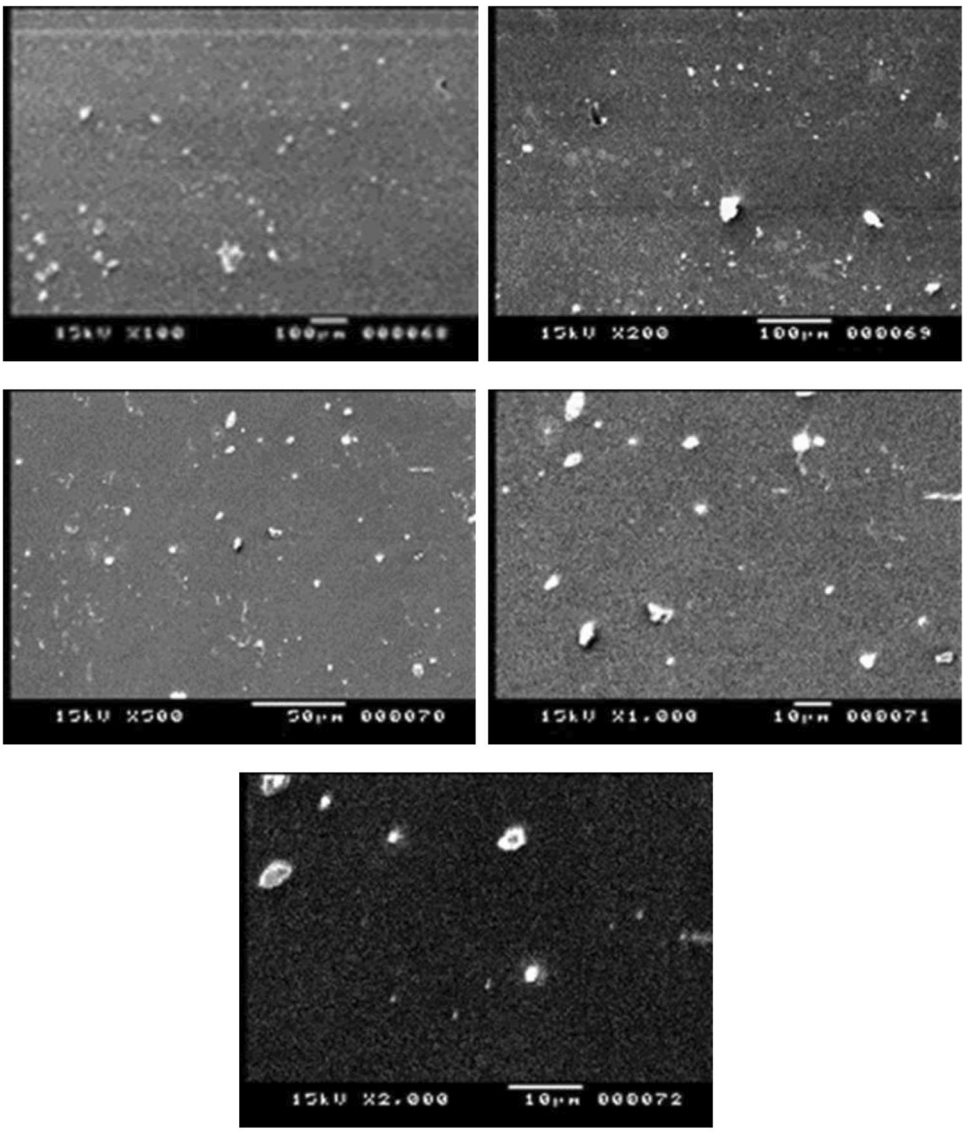

b

fine-grained texture are among the morphological characteristics discovered among the formed crystalline phases. Various precipitated cerium and boron phases are attributed with these different microcrystalline phases throughout heat treatment. The presence of particles with different shapes in both compositions was revealed by SEM micrographs.

3.4 Mechanical Characterization

Non-destructive examinations as ultrasonic can be used to characterize glass–ceramics, investigate their structure, and calculate their elastic constants [56–66]. Figures 15 and 16 show plots of V_L&V_T, as well as elastic moduli ($L, G, K, \& Y$) of the investigated ceramic samples as a function of CeO_2 concentration. As the CeO_2 increases, V_L&V_T, increased. The network's coordination number increased as the mol present of CeO_2 increased, increasing the cross-link density. V_L&V_T were increases due to increase in the packing and connectivity of the glass—ceramic configurations.

Figure 16 shows that as CeO_2 concentrations increased, the elastic moduli $L, G, K, \& Y$ increased. As a result, the observed increase in $L, G, K, \& Y$ with increasing CeO_2 content can be explained by former role of cerium in the ceramic samples. This behavior indicates that the addition of CeO_2 enhanced the packing density and rigidity. Figure 17 depicted (ρ,$H\&d$) of the ceramics sample. Heat treatment increases the (ρ,$H\&d$) of the ceramics investigated. Heat treatment, in my opinion, resulting in some order and compactness. As a result, new properties should originate, and ρ,H should increase. In all ceramic samples, (d) was close to 2 i.e. 2-dimensional layer structure network is present in all the ceramic samples.

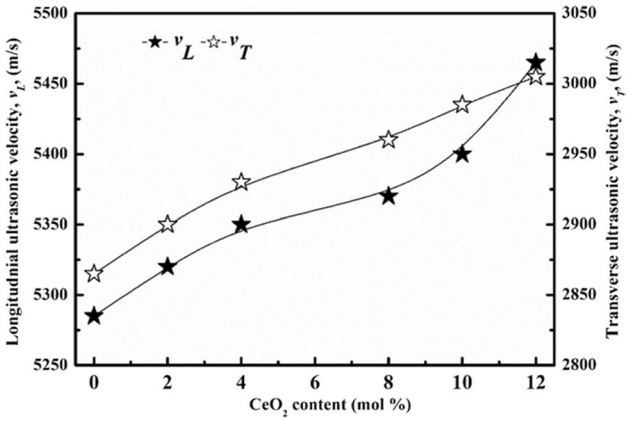

Fig.15 V_L&V_T for glass –ceramic

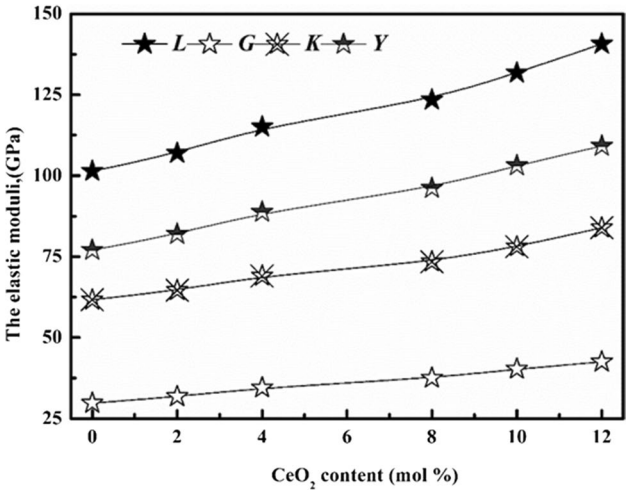

Fig.16 $L, G, K, \& Y$ for glass –ceramic

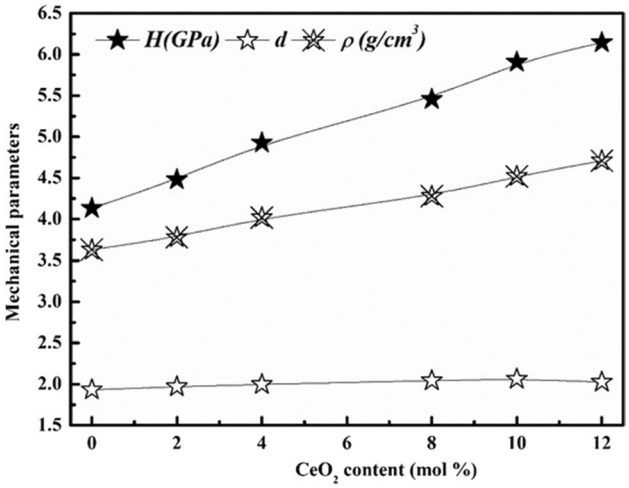

Fig.17 ρ, $H\&d$ for glass -ceramic

4 Conclusions

The combined techniques of DTA, XRD, SEM, and mechanical were used to characterize the thermal behavior and crystallization of CeO_2 co-doped B_2O_3-SiO_2-MoO_3 glasses. The thermal stability of glasses was demonstrated in DTA studies. The quantity of CeO_2 in the checked glass had a significant impact on its crystallization behavior, with an increase in CeO_2 content increasing ΔT and thus making the glasses more stable. With increasing CeO_2 concentrations both E_G & E_c values decreases, as expected rise in T_g & T_p values. The most important aspect of crystalline result characterization is, of course, XRD. XRD measurements were confirmed by mechanical and SEM analysis of crystalline samples. The establishment of glass-crystalline phases in the analysed glass series and the thermal stability of glasses were also revealed by this analysis. This behavior indicates that the addition of CeO_2 enhanced the packing density and rigidity. Therefore, the ultrasonic velocities & elastic moduli increased. Heat treatment, in my opinion, resulting in some order and compactness.

Acknowledgements This work was supported by the King Khalid University through grant RCAMS/KKU/04-22 under the Research Center for Advance Materials (RCAMS) at King Khalid University, Saudi Arabia. The authors express their gratitude to princess Nourah bint Abdulrahman University, Researchers Supporting Project (Grant No. PNURSP2023R32) Princess Nourah bint Abdulrahman University, Riyadh, Saudi Arabia.

Author contributions **Khamies Saber Shaaban,** methodology, writing the manuscript, review the manuscript, and **Badriah Mesfer Alotaibi,** review the manuscript. **Z.A. Alrowaili,** reviews the manuscript **M. S. Al-Buriahi,** review the manuscript, **A.Ashour,** review the manuscript, and **El Sayed Yousef,** review the manuscript.

Data Availability My manuscript and associated personal data.

Declarations

Ethics Approval and Consent to Participate The manuscript has not been published.

Consent to Participate and Publication The authors consent to participate and publication.

Competing Interests The authors declare that they have no known competing financial interests.

References

1. Shaaban KS, Alyousef HA, El-Rehim AFA (2022) CeO_2 Reinforced B_2O_3–SiO_2–MoO_3 Glass System: A Characterization Study Through Physical, Mechanical and Gamma / Neutron Shields Characteristics. Silicon 14:12001–12012. https://doi.org/10.1007/s12633-022-02124-5
2. Shaaban KS, Alotaibi BM, Al-Baradi AM et al (2023) Exploration of the Glass Domain in the SiO_2-B_2O_3-TiO_2-La_2O_3 System. Silicon. https://doi.org/10.1007/s12633-023-02351-4

3. Albarzan B, Almuqrin Aljawhara H, Koubisy MS, Abdel Wahab EA, Mahmoud KA, Shaaban KhS, Sayyed MI (2021) Effect of Fe_2O_3 doping on structural, FTIR and radiation shielding characteristics of aluminium-lead-borate glasses. Prog Nucl Energy 141:103931. https://doi.org/10.1016/j.pnucene.2021.103931
4. Wahab EAA, Alyousef HA, El-Rehim AFA et al (2023) Basicity, Optical Features, and Neutron/Charged Particle Attenuation Characteristics of P_2O_5-As_2O_3-PbO Glasses Doped with Tungsten Ions. J Electron Mater 52:219–236. https://doi.org/10.1007/s11664-022-09969-x
5. Somaily HH, Shaaban KS, Makhlouf SA, Algarni H, Hegazy HH, Wahab EAA, Shaaban ER (2021) Comparative Studies on Polarizability, Optical Basicity and Optical Properties of Lead Borosilicate Modified with Titania. J Inorg Organomet Polym Mater 31:138–150. https://doi.org/10.1007/s10904-020-01650-2
6. Shaaban KS, Alotaibi BM, Alharbiy N et al (2022) Impact of TiO_2 on DTA and Elastic Moduli of Calcium Potassium Borophosphosilicate Glasses in Prelude for Use in Dental and Orthopedic Applications. Silicon 14:11991–12000. https://doi.org/10.1007/s12633-022-02029-3
7. Shaaban KS, Alyousef HA, Alotaibi BM et al (2022) The Vital Role of TiO_2 on the Bioglass System P_2O_5-CaO-B_2O_3-SiO_2- K_2O for Optics and Shielding Characteristics. J Inorg Organomet Polym 32:4295–4303. https://doi.org/10.1007/s10904-022-02446-2
8. Shaaban KS, Al-Baradi AM, Ali AM (2022) Physical, Mechanical, and Thermal Characteristics of B_2O_3 - SiO_2- Li_2O -Fe_2O_3 Glasses. Silicon 14:9609–9616. https://doi.org/10.1007/s12633-022-01703-w
9. Wahab EAA, Al-Baradi AM, Sayed MA et al (2022) Crystallization and Radiation Proficiency of Transparent Sodium Silicate Glass Doped Zirconia. Silicon 14:8581–8597. https://doi.org/10.1007/s12633-021-01652-w
10. Shaaban KS, Al-Baradi AM, Ali AM (2022) Gamma-ray shielding and mechanical characteristics of iron-doped lead phosphosilicate glasses. Silicon 14:8971–8979. https://doi.org/10.1007/s12633-022-01702-x
11. Algarni SA, El-Maaref AA, Alotaibi BM et al (2022) Physical, Optical, and Radiation Shielding Features of Yttrium Lithium Borate Glasses. J Inorg Organomet Polym 32:2873–2881. https://doi.org/10.1007/s10904-022-02321-0
12. El-Maaref AA, Alotaibi BM, Alharbi N et al (2022) Effect of Fe_2O_3 as an Aggregate Replacement on Mechanical, and Gamma/Neutron Radiation Shielding Properties of Phosphoaluminate Glasses. J Inorg Organomet Polym 32:3117–3127. https://doi.org/10.1007/s10904-022-02345-6
13. Shaaban KS, Alrowaili ZA, Al-Baradi AM et al (2022) Mechanical and Thermodynamic Characteristics of 22SiO_2-23Bi_2O_3-37B_2O3-13TiO_2-(5–x) LiF- x BaO Glasses. Silicon 14:6457–6465. https://doi.org/10.1007/s12633-021-01441-5
14. Alomairy S, Alrowaili ZA, Kebaili I et al (2022) Synthesis of Pb_3O_4-SiO_2-ZnO-WO_3 Glasses and their Fundamental Properties for Gamma Shielding Applications. Silicon 14:5661–5671. https://doi.org/10.1007/s12633-021-01347-2
15. Ali AM, Alrowaili ZA, Al-Baradi AM et al (2022) A Study of Thermal, and Optical Properties of 22SiO_2-23Bi_2O_3-37B_2O3-13TiO_2-(5–x) LiF- x BaO Glasses. Silicon 14:6447–6455. https://doi.org/10.1007/s12633-021-01440-6
16. Wahab EAA, Shaaban KS, Al-Baradi AM (2022) Enhancement of Optical and Physical Parameters of Lead Zinc Silicate Glasses by Doping W^{+3} Ions. Silicon 14:4915–4924. https://doi.org/10.1007/s12633-021-01236-8
17. Shaaban KhS, Al-Baradi Ateyyah M, Ali AtifMossad, Alotaibi BM (2022) Thermal, optical, and gamma/ neutron radiation absorption of PbO - P_2O_5 –SiO_2 - Na_2O - Fe_2O_3 glasses. J Mater Res Technol 18:1909–1921. https://doi.org/10.1016/j.jmrt.2022.03.090
18. Shaaban KS, Alotaibi BM, Alharbiy N et al (2022) Fabrication of lithium borosilicate glasses containing Fe_2O_3 and ZnO for FT-IR, UV–Vis–NIR, DTA, and highly efficient shield. Appl Phys A 128:333. https://doi.org/10.1007/s00339-022-05474-4
19. Shaaban KhS, Alotaibi BM, NuhaAlharbi A, Alrowaili ZA, Al-Buriahi MS, Makhlouf SA, Abd El-Rehim AF (2022) Physical, optical, and radiation characteristics of bioactive glasses for dental prosthetics and orthopaedic implants applications. Radiat Phys Chem 193:109995. https://doi.org/10.1016/j.radphyschem.2022.109995
20. Shaaban KS, Alotaibi BM, Algarni SA et al (2022) Chemical Composition, Mechanical, and Thermal Characteristics of Bioactive Glass for Better Processing Features. Silicon 14:10817–10826. https://doi.org/10.1007/s12633-022-01784-7
21. Shaaban KS, Al-Baradi AM, Ali AM (2022) Cr_2O_3 effect on the structure, optical, and radiation shielding properties of $Na_2B_4O_7$–SiO_2–CaO–Cr_2O_3 glasses. Appl Phys A 128:208. https://doi.org/10.1007/s00339-022-05348-9
22. Shaaban KS, Al-Baradi AM, Ali AM (2022) Physical, optical, and advanced radiation absorption characteristics of cadmium lead phosphate glasses containing MoO_3. J Mater Sci Mater Electron 33:3297–3305. https://doi.org/10.1007/s10854-021-07530-w
23. Shaaban KS, Al-Baradi AM, Ali AM (2022) Investigation of BaO reinforced TiO_2–p_2O_5–li_2O glasses for optical and neutron shielding applications. RSC Adv 12:3036–3043. https://doi.org/10.1039/d2ra00171c
24. Alrowaili ZA, Al-Baradi AM, Sayed MA, Ali AM, Abdel Wahab EA, Al-Buriahi MS, Shaaban KhS (2022) The impact of Fe_2O_3 on the dispersion parameters and gamma/fast neutron shielding characteristics of lithium borosilicate glasses. Optik 249:168259. https://doi.org/10.1016/j.ijleo.2021.168259
25. Ali ZAM, Al-Baradi MA, Al-Buriahi MS, Wahab EA, Shaaban KS (2022) A significant role of MoO_3 on the optical, thermal, and radiation shielding characteristics of B_2O_3–P_2O_5–Li_2O glasses. Opt Quant Electr 54:88
26. Shaaban KS, Al-Baradi AM, Alrowaili ZA et al (2021) Structural, thermal, and mechanical characteristics of yttrium lithium borate glasses and glass–ceramics. J Mater Sci Mater Electron 32:28065–28075. https://doi.org/10.1007/s10854-021-07158-w
27 Abdel Wahab EA, Shaaban KS (2021) Structural and optical features of aluminum lead borate glass doped with Fe2O3. Appl Phys A. 127:956. https://doi.org/10.1007/s00339-021-05062-y
28. Alomairy S, Aboraia AM, Shaaban ER et al (2021) Comparative Studies on Spectroscopic and Crystallization Properties of Al_2O_3 -Li_2O- B_2O_3-TiO_2 Glasses. Braz J Phys 51:1237–1248. https://doi.org/10.1007/s13538-021-00928-1
29. Almuqrin AH, Mahmoud KA, Wahab EAA et al (2021) Structural, mechanical, and nuclear radiation shielding properties of iron aluminoleadborate glasses. Eur Phys J Plus 136:639. https://doi.org/10.1140/epjp/s13360-021-01564-z
30. El-Rehim AFA, Ali AM, Zahran HY et al (2021) Spectroscopic, Structural, Thermal, and Mechanical Properties of B_2O_3-CeO_2-PbO_2 Glasses. J Inorg Organomet Polym 31:1774–1786. https://doi.org/10.1007/s10904-020-01799-w
31. El-Rehim AFA, Zahran HY, Yahia IS, Makhlouf SA, Shaaban KS (2021) Radiation, Crystallization, and Physical Properties of Cadmium Borate Glasses. Silicon 13:2289–2307. https://doi.org/10.1007/s12633-020-00798-3
32 El-Rehim AFA, Wahab EAA, Halaka MMA, Shaaban KS (2022) Optical Properties of SiO2 – TiO2 – La2O3 – Na2O – Y2O3 Glasses and A Novel Process of Preparing the Parent Glass-Ceramics. Silicon 14:373–384. https://doi.org/10.1007/s12633-021-01002-w
33. Fayad AM, Shaaban KS, Abd-Allah WM, Ouis M (2020) Structural and Optical Study of CoO Doping in Borophosphate Host Glass and Effect of Gamma Irradiation. J Inorg Organomet Polym Mater 30:5042–5052. https://doi.org/10.1007/s10904-020-01641-3

34. Shaaban KS, Boukhris I, Kebaili I, Al-Buriahi MS (2022) Spectroscopic and Attenuation Shielding Studies on B_2O_3-SiO2-LiF-ZnO-TiO_2 Glasses. Silicon 14:3091–3100. https://doi.org/10.1007/s12633-021-01080-w
35. Mahmoud KH, Elsayed KA, Wahab EAA, Abdel-Rahim FM, Shaaban KS (2021) Structural and radiation shielding simulation of B_2O_3–SiO_2–LiF–ZnO–TiO_2 glasses. J Mater Sci Mater Electron 32:16182–16193. https://doi.org/10.1007/s10854-021-06165-1
36 Abdel Wahab EA, Koubisy MSI, Sayyed MI, Mahmoud KA, Zatsepin AF, Makhlouf SA, Shaaban KS (2021) Novel borosilicate glass system: $Na_2B_4O_7$-SiO_2-MnO_2: Synthesis, average electronics polarizability, optical basicity, and gamma-ray shielding features. J Non-Crystal Solids 553:120509. https://doi.org/10.1016/j.jnoncrysol.2020.120509
37. El-Rehim AFA, Zahran HY, Yahia IS, Ali AM, Shaaban KS (2022) Physical, Radiation Shielding and Crystallization Properties of Na_2O-Bi_2O_3- MoO_3-B_2O_3- SiO_2-Fe_2O_3 Glasses. Silicon 14:405–418. https://doi.org/10.1007/s12633-020-00827-1
38. Mahmoud KH, Alsubaie AS, Wahab EAA, Abdel-Rahim FM, Shaaban KS (2022) Research on the Effects of Yttrium on Bismuth Titanate Borosilicate Glass System. Silicon 14:3419–3427. https://doi.org/10.1007/s12633-021-01125-0
39. Shaaban KS, Al-Baradi AM, Wahab EAA (2022) The Impact of Y_2O_3 on Physical and Optical Characteristics, Polarizability, Optical Basicity, and Dispersion Parameters of B_2O_3 – SiO_2 – Bi_2O_3 – TiO_2 Glasses. Silicon 14:5057–5065. https://doi.org/10.1007/s12633-021-01309-8
40. Al-Baradi AM, Wahab EAA, Shaaban KS (2022) Preparation and Characteristics of B_2O_3 – SiO_2 – Bi_2O_3 – TiO_2 – Y_2O_3 Glasses and Glass-Ceramics. Silicon 14:5277–5287. https://doi.org/10.1007/s12633-021-01286-y
41. Shaaban KS, Alomairy S, Al-Buriahi MS (2021) Optical, thermal and radiation shielding properties of B_2O_3–NaF–PbO–BaO–La_2O_3 glasses. J Mater Sci Mater Electron 32:26034–26048. https://doi.org/10.1007/s10854-021-05885-8
42. El-Maaref AA, Wahab EAA, Shaaban KS, El-Agmy RM (2021) Enhancement of spectroscopic parameters of Er^{3+}-doped cadmium lithium gadolinium silicate glasses as an active medium for lasers and optical amplifiers in the NIR-region. Solid State Sci 113:106539. https://doi.org/10.1016/j.solidstatesciences.2021.106539
43. El-Rehim AFA, Zahran HY, Yahia IS, Wahab EAA, Shaaban KS (2021) Structural, Elastic Moduli, and Radiation Shielding of SiO_2-TiO_2-La_2O_3-Na_2O Glasses Containing $_{Y2O3}$. J Mater Eng Perform 30:1872–1884. https://doi.org/10.1007/s11665-021-05513-w
44. Shaaban KS, Saddeek YB (2017) Effect of MoO_3 Content on Structural, Thermal, Mechanical and Optical Properties of (B_2O_3-SiO_2-Bi_2O_3-Na_2O-Fe_2O_3) Glass System. Silicon 9:785–793. https://doi.org/10.1007/s12633-017-9558-5
45. Shaaban KS, Abo-Naf SM, Hassouna MEM (2019) Physical and Structural Properties of Lithium Borate Glasses Containing MoO_3. Silicon 11:2421–2428. https://doi.org/10.1007/s12633-016-9519-4
46. Shaaban KS, Wahab EAA, Shaaban ER, Yousef ES, Mahmoud SA (2020) Electronic Polarizability, Optical Basicity, Thermal, Mechanical and Optical Investigations of ($65B_2O_3$–$30Li_2O$–$5Al_2O_3$) Glasses Doped with Titanate. J Electron Mater 49:2040–2049. https://doi.org/10.1007/s11664-019-07889-x
47. Sayed MA, Ali AM, Abd El-Rehim AF, Abdel Wahab EA, Shaaban KS (2021) Dispersion Parameters, Polarizability, and Basicity of Lithium Phosphate Glasses. J Electron Mater 50:3116–3128. https://doi.org/10.1007/s11664-021-08921-9
48 Öz B, Öveçoğlu LM, Kabalcı I, Özen G (2007) Microstructural characterization and crystallization kinetics of (1–x)TeO_2–xK_2O (x=0.05, 0.10, 0.15, 0.20mol) glasses. J Eur Ceram Soc 27(10):3239–3251. https://doi.org/10.1016/j.jeurceramsoc.2007.01.010
49 Kabalci I, Özen G, Öveçoğlu ML, Sennaroğlu A (2006) Thermal study and linear optical properties of (1–x)TeO_2–(x)PbF_2 (x=0.10, 0.15 and 0.25mol) glasses. J Alloys Compounds 419(1–2):294–298. https://doi.org/10.1016/j.jallcom.2005.09.062
50. Kabalci I, Koc E, Ozturk SS (2017) Mechanical, Structural and Thermal Properties of Transparent Bi_2O_3–Al_2O_3–ZnO–TeO_2 Glass System. J Inorg Organomet Polym Mater 27:788–794. https://doi.org/10.1007/s10904-017-0523-y
51. Lasocka M (1976) The effect of scanning rate on glass transition temperature of splat cooled $Te_{85}Ge_{15}$. Mater Sci Eng 23:173–177
52. Shaaban KS, Yousef ES (2020) Optical properties of Bi_2O_3 doped boro tellurite glasses and glass ceramics. Optik 203:163976. https://doi.org/10.1016/j.ijleo.2019.163976
53. Shaaban KS, Yousef ES, Abdel Wahab EA, Shaaban ER, Mahmoud SA (2020) Investigation of Crystallization and Mechanical Characteristics of Glass and Glass-Ceramic with the Compositions xFe_2O_3-35SiO_2-35B_2O_3-10Al_2O_3-(20–x) Na_2O. J Mater Eng Perform 29:4549–4558. https://doi.org/10.1007/s11665-020-04969-6
54. Shaaban KS, Abo-Naf SM, Abd Elnaeim AM, Hassouna MEM (2017) Studying effect of MoO_3 on elastic and crystallization behavior of lithium diborate glasses. Applied Physics A 123. https://doi.org/10.1007/s00339-017-1052-9
55. Shaaban KS, Yousef ES, Mahmoud SA, Wahab EAA, Shaaban ER (2020) Mechanical, Structural and Crystallization Properties in Titanate Doped Phosphate Glasses. J Inorg Organomet Polym Mater 30:4655–4663. https://doi.org/10.1007/s10904-020-01574-x
56 Abdel Wahab EA, Shaaban KS, Yousef ES (2020) Enhancement of optical and mechanical properties of sodium silicate glasses using zirconia. Opt Quant Electron 52:458. https://doi.org/10.1007/s11082-020-02575-3
57. Rammah YS, El-Agawany FI, Abdel Wahab EA, Hessien MM, Shaaban KhS (2022) Significant impact of V_2O_5 content on lead phosphor-arsenate glasses for mechanical and radiation shielding applications. Radiat Phys Chem. 193:109956. https://doi.org/10.1016/j.radphyschem.2021.109956
58. El-Rehim AFA, Shaaban KS (2021) Influence of La_2O_3 content on the structural, mechanical, and radiation-shielding properties of sodium fluoro lead barium borate glasses. J Mater Sci Mater Electron 32:4651–4671. https://doi.org/10.1007/s10854-020-05204-7
59. El-Rehim AFA, Shaaban KS, Zahran HY, Yahia IS, Ali AM, Halaka MMA, Makhlouf SA, Wahab EAA, Shaaban ER (2021) Structural and Mechanical Properties of Lithium Bismuth Borate Glasses Containing Molybdenum (LBBM) Together with their Glass-Ceramics. J Inorg Organomet Polym Mater 31:1057–1065. https://doi.org/10.1007/s10904-020-01708-1
60. Mahmoud M, Makhlouf SA, Alshahrani B, Yakout HA, Shaaban KS, Wahab EAA (2022) Experimental and Simulation Investigations of Mechanical Properties and Gamma Radiation Shielding of Lithium Cadmium Gadolinium Silicate Glasses Doped Erbium Ions. Silicon 14:2905–2919. https://doi.org/10.1007/s12633-021-01062-y
61. Shaaban KS, Saddeek YB, Sayed MA, Yahia IS (2018) Mechanical and Thermal Properties of Lead Borate Glasses Containing CaO and NaF. Silicon 10:1973–1978. https://doi.org/10.1007/s12633-017-9709-8
62. Shaaban KS, Zahran HY, Yahia IS, Elsaeedy HI, Shaaban ER, Makhlouf SA, Wahab EAA, Yousef ES (2020) Mechanical and radiation-shielding properties of B_2O_3–P_2O_5–Li_2O–MoO_3 glasses. Appl Phys A 126. https://doi.org/10.1007/s00339-020-03982-9
63. Shaaban KhS, Al-Baradi Ateyyah M, Alotaibi BM, Abd El-Rehim AF (2023) Mechanical and radiation shielding features of lithium titanophosphate glasses doped BaO. J Mater Res Technol. 23:756–764. https://doi.org/10.1016/j.jmrt.2023.01.062
64. Shaaban KS, Alotaibi BM, Yousef ES (2023) Effect of La_2O_3 Concentration on the Structural, Optical and Radiation-Shielding Behaviors of Titanate Borosilicate Glasses. J Electron Mater. https://doi.org/10.1007/s11664-023-10347-4

65. Shaaban KS, Al-Baradi AM, Ali AM (2022) The Impact of Cr_2O_3 on the Mechanical, Physical, and Radiation Shielding Characteristics of $Na_2B_4O_7$–CaO–SiO_2 Glasses. Silicon 14:10375–10382. https://doi.org/10.1007/s12633-022-01783-8
66. Chen C, Zhu Q, Wang H, Huang F, Yang Q, Xu S (2021) Excellent Mechanical Properties of the Silicate Glasses Modified by CeO_2 and TiO_2: a New Choice for High-Strength and High-Modulus Glass Fibers. Silicon. https://doi.org/10.1007/s12633-021-01215-z